catalysts

MDPI

Article

Mechanistic Analysis of Water Oxidation Catalyst *cis*-$[Ru(bpy)_2(H_2O)_2]^{2+}$: Effect of Dimerization

Darren Erdman †, Yuliana Pineda-Galvan † and Yulia Pushkar *

Department of Physics and Astronomy, Purdue University, 525 Northwestern Avenue, West Lafayette, IN 47907, USA; derdman@purdue.edu (D.E.); ypineda@purdue.edu (Y.P.-G.)

* Correspondence: ypushkar@purdue.edu; Tel.: +1-765-496-3279

† These authors contributed equally to this work.

Academic Editors: Albert Demonceau, Ileana Dragutan and Valerian Dragutan

Received: 27 November 2016; Accepted: 18 January 2017; Published: 25 January 2017

Abstract: While the catalytic activity of some Ru-based polypyridine complexes in water oxidation is well established, the relationship between their chemical structure and activity is less known. In this work, the single site Ru complex $[Ru(bpy)_2(H_2O)_2]^{2+}$ (bpy = 2,2′-bipyridine)—which can exist as either a *cis* isomer or a *trans* isomer—is investigated. While a difference in the catalytic activity of these two isomers is well established, with *cis*-$[Ru(bpy)_2(H_2O)_2]^{2+}$ being much more active, no mechanistic explanation of this fact has been presented. The oxygen evolving capability of both isomers at multiple concentrations has been investigated, with *cis*-$[Ru(bpy)_2(H_2O)_2]^{2+}$ showing a second-order dependence of O_2 evolution activity with increased catalyst concentration. Measurement of the electron paramagnetic resonance (EPR) spectrum of *cis*-$[Ru(bpy)_2(H_2O)_2]^{2+}$, shortly after oxidation with Ce^{IV}, showed the presence of a signal matching that of *cis*,*cis*-$[Ru^{III}(bpy)_2(H_2O)ORu^{IV}(bpy)_2(OH)]^{4+}$, also known as "blue dimer". The formation of dimers is a concentration-dependent process, which could serve to explain the greater than first order increase in catalytic activity. The *trans* isomer showed a first-order dependence of O_2 evolution on catalyst concentration. Behavior of $[Ru(bpy)_2(H_2O)_2]^{2+}$ isomers is compared with other Ru-based catalysts, in particular $[Ru(tpy)(bpy)(H_2O)]^{2+}$ (tpy = 2,2′;6,2″-terpyridine).

Keywords: Ru complexes; catalysis of water oxidation; density functional theory; X-band EPR spectroscopy; oxygen evolution; H-bond; dimer formation

1. Introduction

The oxidation of water is a vital reaction in nature, occurring during photosynthesis and as a key step in solar energy conversion schemes centered around artificial photosynthesis. There are numerous water oxidation catalysts (WOC's) that have been reported, many of which are based on transition metals, such as Ir [1,2] and Ru. In attempts to create more economically-viable catalysts, complexes containing more abundant elements such as Fe, Co, and Ni have been discovered [3]. Ru-based WOCs, in particular, have been investigated for decades, and today they are still the most extensively studied group of WOCs. Currently there are many mono-Ru [4–7] and di-Ru [8–11] complexes capable of oxidizing water; however, the stability of molecular catalysts in highly oxidizing conditions is still a major issue, with most known catalysts deactivating after some time [12]. Under strongly oxidizing conditions one of the reaction pathways for single-site complexes involves the formation of dinuclear complexes [13–15]. In some cases, the dinuclear complexes are more stable than their mononuclear counterparts, with the mononuclear catalyst being converted to a binuclear or multinuclear catalyst [13,15].

This work is focused on the study of water oxidation by the single-site complex *cis*-$[Ru(bpy)_2(H_2O)_2]^{2+}$ and electron paramagnetic resonance (EPR) characterization of the products.

Both *cis*- and *trans*-$[Ru(bpy)_2(H_2O)_2]^{2+}$ were reported and characterized by Meyer et al. [16,17]. It was found that the *cis* configuration is more stable in the absence of light, but under illumination the complex undergoes *cis-trans* isomerization. Later, it was shown that upon addition of Ce^{IV}, *cis*-$[Ru(bpy)_2(H_2O)_2]^{2+}$ acts as a water oxidation catalyst, yet its performance is limited by having few turnovers [18]. Interestingly, in the same work, *trans*-$[Ru(bpy)_2(H_2O)_2]^{2+}$ was shown to be a much less active catalyst than *cis*-$[Ru(bpy)_2(H_2O)_2]^{2+}$. The catalytic mechanism of *cis*-$[Ru(bpy)_2(H_2O)_2]^{2+}$ is believed to involve a water nucleophilic attack on the Ru^{V}=O species produced in a series of proton-coupled electron transfer reactions, which occur upon oxidation [18]. *cis*-$[Ru(bpy)_2(H_2O)_2]^{2+}$ and various products of its oxidation have been studied by density functional theory (DFT), EPR, and X-ray Absorption Spectroscopy, allowing for the establishment of their geometric and electronic structure [19].

Here, we report our study of water oxidation at acidic conditions, using $[Ru(bpy)_2(H_2O)_2]^{2+}$ as a catalyst upon addition of Ce^{IV}. It was found that for the more catalytically active *cis* isomer, the rate of O_2 evolution increases non-linearly with complex concentration. This effect is ascribed to the formation of a di-Ru complex of $[Ru(bpy)_2(H_2O)_2]^{2+}$. EPR signals of the *cis*-$[Ru^{V}(bpy)_2(O)(OH)]^{2+}$ species and *cis*,*cis*-$[Ru^{III}(bpy)_2(H_2O)ORu^{IV}(bpy)_2(OH)]^{4+}$ dimer resulting from its reactivity are reported. DFT calculations were used to show that dimer formation is energetically favorable. While on a much slower time scale, dimer formation during catalysis has previously been reported for $[Ru(tpy)(bpy)(H_2O)]^{2+}$ [13,14] and so a comparison of the two compounds is provided.

2. Results

2.1. Oxygen Evolution Measurements

The oxygen evolving activity of *cis*-$[Ru(bpy)_2(H_2O)_2]^{2+}$ was assessed at acidic pH = 1 (0.1 M HNO_3) using a Clark electrode. To induce O_2 evolution, an excess (20 equiv.) of Ce^{IV} oxidant was added. Figure 1A shows the resulting O_2 evolution profiles for different concentrations (0.2–1 mM) of *cis*-$[Ru(bpy)_2(H_2O)_2]^{2+}$. There was a delay between injecting Ce^{IV} and an increase in O_2 concentration which is greater at lower concentrations of $[Ru(bpy)_2(H_2O)_2]^{2+}$ (0.2–0.4 mM). Additionally, it is evident that at given conditions (20 equiv. Ce^{IV}, in 0.1 M HNO_3), the rate of oxygen evolution increased non-linearly with complex concentration. The initial rate was determined within the first 15 s of the oxygen evolution, and was plotted against the concentration of *cis*-$[Ru(bpy)_2(H_2O)_2]^{2+}$ (Figure 1B). Oxygen evolution measurements show that the rate of oxygen production had a second order dependence on the concentration of the complex. These results indicate that there could be a secondary concentration-dependent process occurring upon the addition of Ce^{IV}.

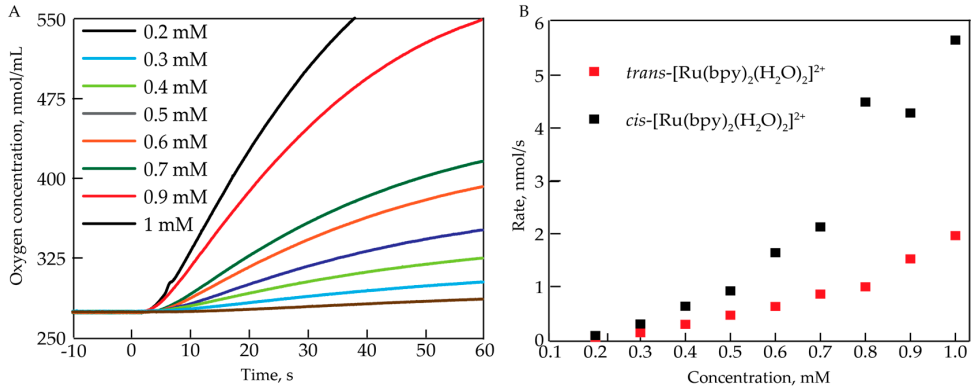

Figure 1. (**A**) Oxygen evolution profiles for different concentrations of *cis*-$[Ru(bpy)_2(H_2O)_2]^{2+}$ in 0.1 M HNO_3. 20 equiv. of Ce^{IV} were added at t = 0 s; (**B**) Initial rate (determined between 5 and 10 s) of O_2 evolution as a function of the complex concentration for *cis*-$[Ru(bpy)_2(H_2O)_2]^{2+}$ and *trans*-$[Ru(bpy)_2(H_2O)_2]^{2+}$.

Figure 2 compares the oxygen evolution profiles at a 0.7 mM concentration of *cis*-$[Ru(bpy)_2(H_2O)_2]^{2+}$ and $[Ru(tpy)(bpy)(H_2O)]^{2+}$, which is one of the most extensively characterized single-site water oxidation catalysts. It is clear that the two seemingly similar single-site catalysts have significantly different catalytic activity.

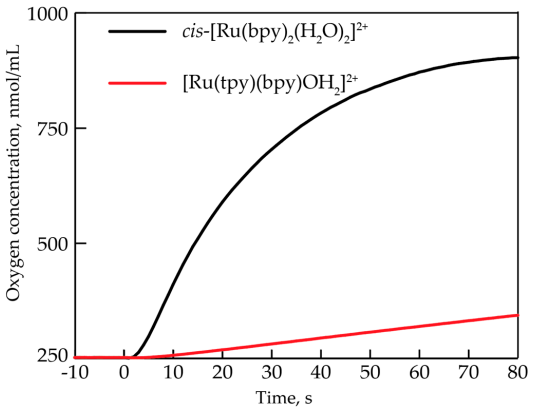

Figure 2. Oxygen evolution profiles of *cis*-$[Ru(bpy)_2(H_2O)_2]^{2+}$ (black) and $[Ru(tpy)(bpy)(H_2O)]^{2+}$ upon the addition of 20 equiv. Ce^{IV}. Conditions: room temperature, 0.7 mM concentration of Ru complex, 0.1 M HNO_3 (pH = 1).

2.2. Electron Paramagnetic Resonance Measurements

Studies using EPR were done to identify the products of the reaction. Oxidized samples were frozen within 30 s after the addition of Ce^{IV}, and their EPR spectra were measured. The samples were then melted at room temperature for 2 min, refrozen and another set of EPR spectra was obtained. Figure 3A shows EPR spectra obtained after oxidizing 200 µL of 1 mM $[Ru(bpy)_2(H_2O)_2]^{2+}$ with 2–20 equiv. of Ce^{IV} and freezing it within 30 s. There was a rhombic EPR signal observed with g_{xx} = 2.05, g_{yy} = 1.99 and g_{zz} = 1.85. Its maximum intensity was observed upon adding 3 equiv. of Ce^{IV}. This signal is characteristic for intermediates containing a Ru^{V}=O fragment [20] and has been previously reported for *cis*-$[Ru(bpy)_2(H_2O)_2]^{2+}$ [19].

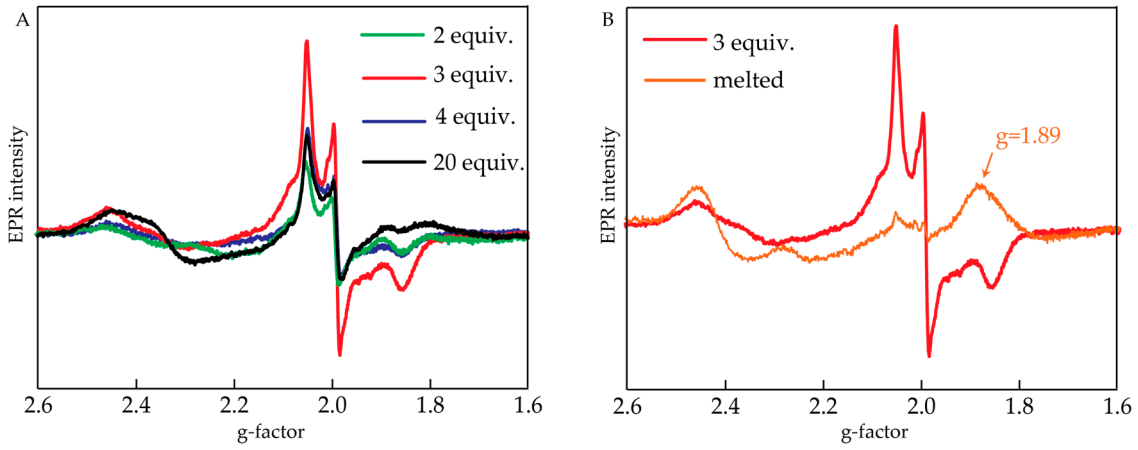

Figure 3. (**A**) Electron paramagnetic resonance (EPR) spectra of *cis*-$[Ru(bpy)_2(H_2O)_2]^{2+}$ upon addition of 2, 3, 4 or 20 equiv. of Ce^{IV} and immediate freezing of the sample; (**B**) EPR spectrum of *cis*-$[Ru(bpy)_2(H_2O)_2]^{2+}$ + 3 equiv. of Ce^{IV} before and after melting for 2 min. Conditions: 20 K, 1 mM *cis*-$[Ru(bpy)_2(H_2O)_2]^{2+}$, 0.1 M HNO_3 (pH = 1).

The sample that was oxidized with 3 equiv. of Ce^{IV} was melted for 2 min and then refrozen. The resulting EPR spectrum compared to the one before melting is shown in Figure 3B. First, it is

seen that the signal related to Ru^{V}=O has decreased significantly. A new signal appeared at g = 1.89, which is characteristic of the so-called "blue dimer" (*cis*,*cis*-[$Ru^{III}(bpy)_2(H_2O)ORu^{IV}(bpy)_2(OH)]^{4+}$) complex [21–23]. Same EPR signal was obtained in catalytic mixture produced by adding 20 equiv. of Ce^{IV} (data not shown). This indicates that after short time and at high concentration of the initial catalyst, a di-Ru complex was formed under the conditions of water oxidation.

2.3. Density Functional Theory Calculations

In order to rationalize the difference in the kinetic behavior in the *trans* and *cis* isomers, DFT calculations were done to analyze the intermediates of the water oxidation catalysis, Figures 4 and 5. DFT results show that the short-lived $[(bpy)_2Ru^{V}$=O,OH$]^{2+}$ intermediate detected by EPR was accessible by oxidation with Ce^{IV} at predicted +1.4 V, which is in good agreement with reported experimental redox potential of +1.3 V, Table 1. To analyze pathways for dimerization and radical coupling proposed for some of Ru-based catalysts [24], we computed a $\Delta G = -0.27$ eV for dimer formation from two $[(bpy)_2Ru^{V}$=O,OH$]^{2+}$ molecules (Figure 4). This dimer appears to be stabilized by two hydrogen bonds, which is only possible for the *cis* isomer of the complex (Figure 4). Formation of the peroxo-bridged dimer with O–O bond distance of ~1.34 Å has a $\Delta G = -0.33$ eV, Table 1. After oxygen is expelled from this peroxo-bridged intermediate, there is a possibility of the μ-oxo-bridge formation between two Ru centers, Table 1. The overall reaction leading from the two $[(bpy)_2Ru^{V}$=O,OH$]^{2+}$ molecules to oxygen (O_2) and blue dimer in the oxidation state BD [III,III] has a significant driving force of −1.55 eV, Table 1.

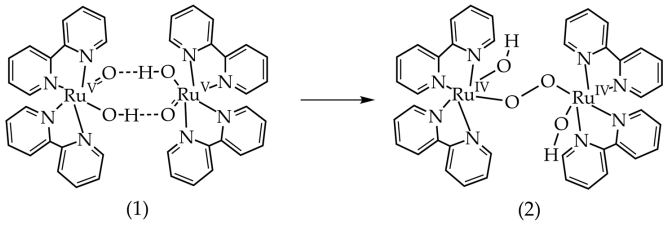

Figure 4. Proposed path with formation of H-bond-stabilized dimer of $[(bpy)_2Ru^{V}$=O,OH$]^{2+}$. The starting compound, (**1**), can only be formed by the *cis* isomer, which could explain the different rates of oxygen production of the two isomers. The optimized geometry of the initial state, (**1**), as well as the product, (**2**), were found.

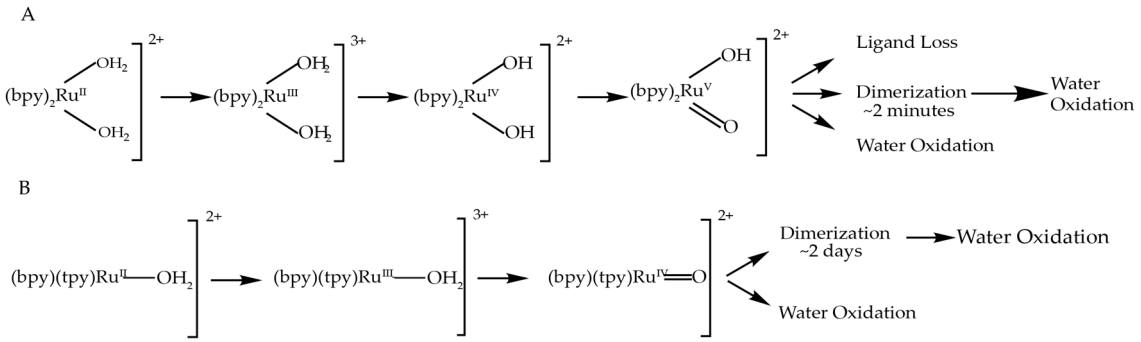

Figure 5. (**A**) Reaction pathway for *cis*-$[Ru^{II}(bpy)_2(H_2O)_2]^{2+}$ up to Ru^{V}, the highest measured oxidation state, and possible paths it follows from there; (**B**) Reaction pathway for *cis*-$[Ru^{II}(bpy)_2(H_2O)_2]^{2+}$ up to Ru^{IV}, the highest measured oxidation state, and possible paths it could follow from there.

From the available experimental observables, we currently cannot determine the relative contributions of the two catalytic mechanisms: catalysis via radical coupling in the dimer of the $[(bpy)_2Ru^{V}$=O,OH$]^{2+}$ versus catalysis derived by the reactivity of the blue dimer, which can be formed in significant amounts after a single turnover. However, it is clear that the *trans* isomer of the

$[Ru(bpy)_2(H_2O)_2]^{2+}$ will be less susceptible to both the dimer formation and the transformation into blue dimer complex.

Table 1. Summary of DFT calculations on the intermediates of *cis*-$[Ru(bpy)_2(H_2O)_2]^{2+}$. Comparison between the calculated redox potential and experimentally reports redox potential is provided, and ΔG for possible dimer formation is shown.

Molecule [1]	Free Energy [2] (kcal/mol)	E^0/V Calculated	E^0/V Experimental
Ru^{II}-$2H_2O$; $2H_2O$	-3.601133×10^6	-	-
Ru^{III}-$2H_2O$; $2H_2O$	-3.601006×10^6	-	-
Ru^{III}-$2H_2O$; $2H_2O + 1e^- = Ru^{II}$-$2H_2O$; $2H_2O$	-	1.04 [25]	0.88 [17]
Ru^{IV}-OH,OH; $2H_2O$	-3.600339×10^6	-	-
Ru^{IV}-OH,OH; $2H_2O + 1e^- + 2H^+ = Ru^{III}$-$2H_2O$; $2H_2O$	-	1.18 [25]	1.19 [17]
Ru^{V}=O,OH; $2H_2O$	-3.599935×10^6	-	-
Ru^{V}=O,OH; $2H_2O + 1e^- + H^+ = Ru^{IV}$-OH,OH; $2H_2O$	-	1.47 [25]	1.34 [17]
Molecule [2]	**Free Energy (kcal/mol)**	**Change in Free Energy (kcal/mol)**	
$H_2ORu^{III}ORu^{III}OH_2$	-6.961716×10^6	-	
O_2	-9.433726×10^4	-	
H_2O	-4.794981×10^4	-	
$2Ru^{V}$=O,OH + $H_2O = H_2ORu^{III}ORu^{III}OH_2 + O_2$	-	−36.04	
$[Ru^{V}$=O,OH$]_2$	-7.008076×10^6	-	
$2Ru^{V}$=O,OH = $[Ru^{V}$=O,-OH$]_2$	-	−6.28	
$HORu^{IV}OORu^{IV}OH$	-7.008084×10^6	-	
$[Ru^{V}$=O,-OH$]_2 = HORu^{IV}OORu^{IV}OH$	-	−7.67	
$HORu^{IV}OORu^{IV}OH + H_2O = H_2ORu^{III}ORu^{III}OH_2 + O_2$	-	−22.09	

[1] All bpy ligands were dropped for clarity; [2] Calculations included two explicit water molecules.

3. Discussion

3.1. Oxygen Evolution by cis-$[Ru(bpy)_2(H_2O)_2]^{2+}$ with DFT and EPR Characterization

The initial report indicated that *cis*-$[Ru(bpy)_2(H_2O)_2]^{2+}$ is unstable, and thus water oxidation is preceded by ligand loss and the formation of RuO_2 [17]. More recent studies have shown a surprising fact: *cis*-$[Ru(bpy)_2(H_2O)_2]^{2+}$ is more active under catalytic conditions, with a turnover number(*TON*) = 4, than *trans*-$[Ru(bpy)_2(H_2O)_2]^{2+}$, with a *TON* = 1. The two complexes showed a significantly different behavior, meaning that, counter to what was proposed in [17]—*cis*-$[Ru(bpy)_2(H_2O)_2]^{2+}$ does not evolve oxygen via ligand loss preceding the formation of RuO_2. If the oxidation of water was occurring due to formation of RuO_2, the lower catalytic activity of the *trans* isomer could be explained by the higher stability of the ligands in the *trans* isomer relative to the *cis* isomer [14]. The TON for *cis*-$[Ru(bpy)_2(H_2O)_2]^{2+}$, however, was shown to be higher than both RuO_2, indicating a need for another explanation. If (as proposed in [13]) the oxidation of water by *cis*-$[Ru(bpy)_2(H_2O)_2]^{2+}$ is accomplished purely by water nucleophilic attack on oxidized form of *cis*-$[Ru(bpy)_2(H_2O)_2]^{2+}$, however, the rate of oxygen evolution should be linear in the concentration of *cis*-$[Ru(bpy)_2(H_2O)_2]^{2+}$. Our oxygen evolution measurements, however, have shown that the O_2 evolution rate has second order dependence on concentration of *cis*-$[Ru(bpy)_2(H_2O)_2]^{2+}$.

Second-order behavior shows that there could be a reaction in the oxidation cycle with a dependence on the concentration of *cis*-$[Ru(bpy)_2(H_2O)_2]^{2+}$. A possible mechanism that would explain a second-order reaction is radical coupling between two Ru^V=O species with the formation of O–O bond ($2Ru^V$=O,OH→HO-Ru^{IV}-O-O-Ru^{IV}-OH), Figure 4. Counter to what was seen with *cis*-$[Ru(bpy)_2(H_2O)_2]^{2+}$, oxygen evolution shows that the rate of oxygen production for *trans*-$[Ru(bpy)_2(H_2O)_2]^{2+}$ is linear in the same concentration range. This indicates that the two isomers are following different reaction mechanisms when oxidized. The requirement for radical coupling to occur is reaching the Ru^V=O complex in the catalytic cycle [24]. While at higher pH, it was shown that only the *cis* isomer is stable in the Ru^V=O configuration, both are able to reach Ru^V at pH 1.0 [17] , where this experiment occurred. If the radical coupling mechanism is taking place for the *cis*-isomer and not the *trans*-isomer, it would explain the difference in catalytic activity, as this pathway corresponds to a high rate of oxygen production. The difference in behavior of the *cis* and

trans isomers means that the radical coupling mechanism (if it is occurring) has to be proceeded by a reaction involving both coordinated oxygens.

It could be that the *cis*-isomer of the complex is forming the blue dimer, either instead of or after the radical coupling pathway. In combination with the linear dependence of the rate of oxygen production on concentration, this process gives a second-order dependence. With EPR analysis, we have seen that *cis*-$[Ru(bpy)_2(H_2O)_2]^{2+}$ is likely forming the so-called "blue dimer" upon adding oxidizing agent. "Blue dimer" is known to be able to oxidize water and in fact was the first designed water oxidation catalyst [8]. The formation of a new catalytically active, di-Ru complex would explain the non-linear dependence of the O_2 evolution rate on concentration. Our oxygen evolution measurements also show that-due to linear dependence on concentration-dimers are not being formed by *trans*-$[Ru(bpy)_2(H_2O)_2]^{2+}$. The oxygen evolution rate of the "blue dimer" complex is about 4.3 nM/s after adding 20 equiv. of Ce^{IV} to 0.1 mM of the complex in 0.1 M HNO_3 [26]. For the *cis*-$[Ru(bpy)_2(H_2O)_2]^{2+}$, oxygen evolution rates range from 0.1 to 5.8 nM/s across the concentration range 0.2–1 mM. So, *cis*-$[Ru(bpy)_2(H_2O)_2]^{2+}$ and blue dimer have comparable oxygen evolution rates at the same oxidation conditions. As the percent of the initial complex converted to blue dimer is unknown, the exact comparison of rates is not possible. More detailed structural studies would need to be done in order to distinguish between formation of H-bonded dimer of $[(bpy)_2Ru^{V}=O,OH]^{2+}$ and formation of blue dimer.

3.2. Comparison to Other Single-Site Ru WOC's

Most single-site Ru WOC's contain polypyridine ligands and one or more water molecules coordinated to the Ru center. $[Ru(tpy)(bpy)(H_2O)]^{2+}$ is a typical representative of this class of catalysts, and has been extensively studied. Highly oxidized intermediates (containing Ru^{IV}=O fragment) are produced via proton-coupled electron transfer (PCET) which requires the presence of a ligand that can be deprotonated (usually water). The derivatives of this complex that do not contain water (or other ligands capable of PCET), such as $[Ru(tpy)(bpy)Cl]^{2+}$ and $[Ru(tpy)(bpy)I]^{2+}$ have been studied. It was demonstrated that the Ru-Cl bond is retained under oxidative conditions, and thus $[Ru(tpy)(bpy)Cl]^{2+}$ is not a water oxidation catalyst [25]. $[Ru(tpy)(bpy)I]^{2+}$ however loses the iodide ligand upon oxidation and forms the same intermediate as the parent complex via PCET, namely $[(tpy)(bpy)Ru^{IV}=O]^{2+}$ [25,27]. This implies at least one Ru-H_2O fragment is required in order for the complex to be an active catalyst.

It has been proposed that $[Ru(tpy)(bpy)(H_2O)]^{2+}$ is capable of forming an intermediate with a high oxidation state, $[(tpy)(bpy)Ru^{V}=O]^{3+}$, and that its reaction with water is the rate-limiting step; however, there is no direct experimental proof that it reaches this oxidation state. Attempts to spectroscopically demonstrate the presence of the Ru^{V}=O intermediate have been unsuccessful, and it has been confirmed by use of X-ray spectroscopy and EPR that in catalytic steady state, the majority of species present are $[(tpy)(bpy)Ru^{IV}=O]^{2+}$ [25]. No Ru^{V}=O species has been directly observed so far for $[Ru(tpy)(bpy)(H_2O)]^{2+}$ or other single-site Ru complexes containing only one water molecule.

$[Ru(bpy)_2(H_2O)_2]^{2+}$, in contrast to $[Ru(tpy)(bpy)(H_2O)]^{2+}$, has 2 water molecules coordinated to Ru center. This makes the formation of Ru^{V}=O fragment possible via PCET, which was observed using EPR spectroscopy in this and previous work [16]. This fact once again demonstrates that the oxidation of Ru center to Ru^{V} via PCET is possible only in the presence of at least 2 ligands capable of deprotonation (i.e., water).

DFT simulations have been performed on $[Ru(tpy)(bpy)(H_2O)]^{2+}$ [25]. They show that the Ru^{V}=O intermediate is much less energetically accessible in $[Ru(tpy)(bpy)(H_2O)]^{2}$ than in $[Ru(bpy)_2(H_2O)_2]^{2+}$ (Table 2), thus supporting the experimental data.

The formation of catalytically active dimers under catalytic conditions has been observed not only for *cis*-$[Ru(bpy)_2(H_2O)_2]^{2+}$, but also for $[Ru(tpy)(bpy)(H_2O)]^{2+}$ and similar complexes [13,14]. It was demonstrated that after prolonged oxidation of $[Ru(tpy)(bpy)(H_2O)]^{2+}$ via bulk electrolysis at 1.64 V (vs. normal hydrogen electrode), a significant part of it is irreversibly converted into a more stable di-nuclear complex that is also capable of oxidizing water. The difference, however, is in the

timescale of the dimerization effect: in the case of *cis*-$[Ru(bpy)_2(H_2O)_2]^{2+}$, the EPR signal characteristic to the di-Ru complex is observed within minutes, while for example $[Ru(tpy)(5,5'\text{-}H_2\text{-}bpmy)(H_2O)]^{2+}$ shows ~25% conversion to its corresponding di-nuclear complex after 2 days of bulk electrolysis. The formation of di-nuclear complexes from $[Ru(tpy)(bpy)(H_2O)]^{2+}$ also requires the loss of bpy ligand by one of the complexes, while *cis*-$[Ru(bpy)_2(H_2O)_2]^{2+}$ does not need to lose a ligand. Figure 4 shows the pathways of both catalysts and products of their oxidation, up to the highest oxidation state measure for each, and the possible outcomes from there.

Table 2. Summary of DFT calculations on the intermediates of $[Ru(tpy)(bpy)(H_2O)]^{2+}$. Comparison between the calculated redox potential and experimentally reports redox potential is provided. Each calculation included two explicit water molecules. Results show a much higher potential for the Ru^{V}=O intermediate as compared to $[Ru(bpy)_2(H_2O)]^{2+}$.

Molecule	Free Energy (kcal/mol)	E^0/V Calculated	E^0/V Experimental
Ru^{II}-H_2O; $2H_2O$	-3.708209×10^6	-	-
Ru^{III}-H_2O; $2H_2O$	-3.708082×10^6	-	-
Ru^{III}-H_2O; $2H_2O$ + $1e^-$ = Ru^{II}-H_2O; $2H_2O$	-	1.06 [25]	1.04 [28]
Ru^{IV}=O; $2H_2O$	-3.707414×10^6	-	-
Ru^{IV}=O; $2H_2O$ + $1e^-$ + $2H^+$ = Ru^{III}-H_2O ; $2H_2O$	-	1.23 [25]	1.39 [28]
Ru^{V}=O; $2H_2O$	-3.707418×10^6	-	-
Ru^{V}=O; $2H_2O$ + $1e^-$ = Ru^{II}-H_2O ; $2H_2O$	-	2.13 [25]	1.60 [5], 1.73 [29], 1.80 [30]

It is also interesting to note that the activities of $[Ru(tpy)(bpy)(H_2O)]^{2+}$ and $[Ru(bpy)_2(H_2O)_2]^{2+}$ are drastically different: it has been previously reported that $[Ru(bpy)_2(H_2O)_2]^{2+}$ is able to do only a few turnovers (*TON* = 4 for *cis* isomer), while $[Ru(tpy)(bpy)(H_2O)]^{2+}$ demonstrates TON on the order of 1000 [31]. It could be explained by the difference in stability of tpy and bpy ligands (the first one has 3 nitrogen atoms coordinated to Ru center while another has only 2); the detailed analysis of stability of these complexes is, however, a subject reserved for a separate study. Despite the similarity in the structure of the two, $[Ru(bpy)_2(H_2O)_2]^{2+}$ is a much more active WOC than $[Ru(tpy)(bpy)(H_2O)]^{2+}$, but with a much shorter lifetime.

4. Materials and Methods

Aqueous solutions were prepared using ultrapure (Type 1) water (resistivity 18.2 MΩ·cm at 25 °C) from a Q-POD unit of Milli-Q integral water purification system (Millipore, Billerica, MA, USA). Solvents and chemicals were purchased from Sigma-Aldrich (St. Louis, MO, USA) and used without further purification.

To prepare *cis*-$[Ru(bpy)_2(H_2O)_2]^{2+}$, 200 mg (0.38 mmol) of *cis*-$[Ru(bpy)_2Cl_2]\cdot 2H_2O$ was dissolved in 30 mL of EtOH. After dissolving, 130 mg (0.76 mmol) of $AgNO_3$ was added. The mixture was refluxed for 30 min. The deposited AgCl was then separated by filtration. The solution's volume was reduced by rotary evaporation, after which 20 mL of H_2O was added. A solution of 125 mg of NH_4PF_6 in 3 mL H_2O was added, immediately forming crystals. The resulting crystals were filtered and washed twice with ethanol and diethyl ether.

X-band EPR measurements were performed on an EMX X-band spectrometer equipped with an X-Band CW microwave bridge (Bruker, Billerica, MA, USA). Samples were oxidized with ammonium cerium nitrate (Ce^{IV}) and frozen within 30 s in liquid nitrogen. During EPR measurements sample temperature was maintained at 20 K using a closed cycle cryostat (ColdEdge Technologies, Allentown, PA, USA). Spectrometer conditions were as follows: microwave frequency 9.47 GHz; field modulation amplitude 10 G at 100 kHz, microwave power 31.7 mW. Measurements were performed on the same day in the same conditions, in order to allow comparison of signal intensities.

Oxygen evolution was measured with Clark type polarographic oxygen electrode with an Oxygraph System (Hansatech Instruments Ltd., King's Lynn, Norfolk, UK). Borosilicate vessel was filled with 600 µL solution of the complex at pH = 1 (in 0.1 M nitric acid) and constantly stirred. Ce^{IV}

dissolved in nitric acid at pH = 1 was added to the chamber and oxygen concentration was recorded as a function of time. Calibration was performed by measuring signal in O_2-saturated deionized water and then adding sodium dithionite (oxygen-depleting agent). Drop in the signal was set equal to the solubility of oxygen in water at room temperature (262 µmol/L).

Density functional theory calculations were performed at the UB3LYP level of theory, with the DGDZVP basis set for the ruthenium atoms, with all other atoms using the 6-31G* basis set. All molecules were modelled in water using the Conductor Polarized Continuum Model (CPCM) solvation model. Additionally, two explicit water molecules were included. All redox potentials were calculated using the DFT calculated free energies of the products minus the reactants. From this value, 4.44 V was subtracted to account for the NHE voltage. The free energy of solvation for H^+ was taken to be −11.64 eV.

Acknowledgments: This material is based upon work supported by the U.S. Department of Energy, Office of Sciences, Office of Basic Energy Sciences under grant number DE-FG02-10ER16184 (Yulia Pushkar) Access to EPR was provided by the Amy Instrumentation Facility, Department of Chemistry, Purdue University, under the supervision of Michael Everly.

Author Contributions: Darren Erdman, Yuliana Pineda-Galvan and Yulia Pushkar performed the experiments, analyzed the data and wrote the paper.

Conflicts of Interest: The authors declare no conflict of interest. The funding sponsors had no role in the design of the study; in the collection, analyses, or interpretation of data; in the writing of the manuscript, and in the decision to publish the results.

References

1. Hull, J.F.; Balcells, D.; Blakemore, J.D.; Incarvito, C.D.; Eisenstein, O.; Brudvig, G.W.; Crabtree, R.H. Highly active and robust Cp* iridium complexes for catalytic water oxidation. *J. Am. Chem. Soc.* **2009**, *131*, 8730–8731. [CrossRef] [PubMed]
2. Blakemore, J.D.; Schley, N.D.; Balcells, D.; Hull, J.F.; Olack, G.W.; Incarvito, C.D.; Eisenstein, O.; Brudvig, G.W.; Crabtree, R.H. Half-sandwich iridium complexes for homogeneous water-oxidation catalysis. *J. Am. Chem. Soc.* **2010**, *132*, 16017–16029. [CrossRef] [PubMed]
3. Wasylenko, D.J.; Palmer, R.D.; Berlinguette, C.P. Homogeneous water oxidation catalysts containing a single metal site. *Chem. Commun.* **2013**, *49*, 218–227. [CrossRef] [PubMed]
4. Zong, R.; Thummel, R.P. A new family of Ru complexes for water oxidation. *J. Am. Chem. Soc.* **2005**, *127*, 12802–12803. [CrossRef] [PubMed]
5. Concepcion, J.J.; Jurss, J.W.; Templeton, J.L.; Meyer, T.J. One site is enough. Catalytic water oxidation by $[Ru(tpy)(bpm)(OH_2)]^{2+}$ and $[Ru(tpy)(bpz)(OH_2)]^{2+}$. *J. Am. Chem. Soc.* **2008**, *130*, 16462–16463. [CrossRef] [PubMed]
6. Kaveevivitchai, N.; Zong, R.; Tseng, H.W.; Chitta, R.; Thummel, R.P. Further observations on water oxidation catalyzed by mononuclear Ru(II) complexes. *Inorg. Chem.* **2012**, *51*, 2930–2939. [CrossRef] [PubMed]
7. Yagi, M.; Tajima, S.; Komia, M.; Yamazakia, H. Highly active and tunable catalysts for O_2 evolution from water based on mononuclear ruthenium(II) monoaquo complexe. *Dalt. Trans.* **2011**, *40*, 3802–3804. [CrossRef] [PubMed]
8. Gersten, S.W.; Samuels, G.J.; Meyer, T.J. Catalytic oxidation of water by an oxo-bridged ruthenium dimer. *J. Am. Chem. Soc.* **1982**, *104*, 4029–4030. [CrossRef]
9. Wada, T.; Tsuge, K.; Tanaka, K. Electrochemical oxidation of water to dioxygen catalyzed by the oxidized form of the bis(ruthenium-hydroxo) complex in H_2O. *Angew. Chemie Int. Ed.* **2000**, *39*, 1479–1482. [CrossRef]
10. Sander, A.C.; Maji, S.; Francàs, L.; Böhnisch, T.; Dechert, S.; Llobet, A.; Meyer, F. Highly efficient binuclear ruthenium catalyst for water oxidation. *ChemSusChem* **2015**, *8*, 1697–1702. [CrossRef] [PubMed]
11. Deng, Z.; Tseng, H.W.; Zong, R.; Wang, D.; Thummel, R. Preparation and study of a family of dinuclear Ru(II) complexes that catalyze the decomposition of water. *Inorg. Chem.* **2008**, *47*, 1835–1848. [CrossRef] [PubMed]
12. Limburg, B.; Bouwman, E.; Bonnet, S. Molecular water oxidation catalysts based on transition metals and their decomposition pathways. *Coord. Chem. Rev.* **2012**, *256*, 1451–1467. [CrossRef]

13. López, I.; Ertem, M.Z.; Maji, S.; Benet-Buchholz, J.; Keidel, A.; Kuhlmann, U.; Hildebrandt, P.; Cramer, C.J.; Batista, V.S.; Llobet, A. A self-improved water-oxidation catalyst: Is one site really enough? *Angew. Chemie Int. Ed.* **2014**, *126*, 209–213. [CrossRef]
14. López, I.; Maji, S.; Benet-Buchholz, J.; Llobet, A. Oxo-bridge scenario behind single-site water-oxidation catalysts. *Inorg. Chem.* **2015**, *54*, 658–666. [CrossRef] [PubMed]
15. Tsubonouchi, Y.; Lin, S.; Parent, A.R.; Brudvig, G.W.; Sakai, K. Light-induced water oxidation catalyzed by an oxido-bridged triruthenium complex with a Ru–O–Ru–O–Ru motif. *Chem. Commun.* **2016**, *52*, 8018–8021. [CrossRef] [PubMed]
16. Durham, B.; Wilson, S.R.; Hodgson, D.J.; Meyer, T.J. Cis-trans photoisomerization in $Ru(bpy)_2(OH_2)_2^{2+}$. Crystal structure of trans-$[Ru(bpy)_2(OH_2)(OH)](ClO_4)_2$. *J. Am. Chem. Soc.* **1980**, *102*, 600–607. [CrossRef]
17. Dobson, J.C.; Meyer, T.J. Redox properties and ligand loss chemistry in aqua/hydroxo/oxo complexes derived from *cis*-and *trans*-$[(bpy)_2Ru^{II}(OH_2)_2]^{2+}$. *Inorg. Chem.* **1988**, *27*, 3283–3291. [CrossRef]
18. Sala, X.; Ertem, M.Z.; Vigara, L.; Todorova, T.K.; Chen, W.; Rocha, R.C.; Aquilante, F.; Cramer, C.J.; Gagliardi, L.; Llobet, A. The *cis*-$[Ru^{II}(bpy)_2(H_2O)_2]^{2+}$ water-oxidation catalyst revisited. *Angew. Chemie Int. Ed.* **2010**, *49*, 7745–7747. [CrossRef] [PubMed]
19. Planas, N.; Vigara, L.; Cady, C.; Miró, P.; Huang, P.; Hammarström, L.; Styring, S.; Leidel, N.; Dau, H.; Haumann, M.; et al. Electronic structure of oxidized complexes derived from *cis*-$[Ru^{II}(bpy)_2(H_2O)_2]^{2+}$ and its photoisomerization mechanism. *Inorg. Chem.* **2011**, *50*, 11134–11142. [CrossRef] [PubMed]
20. Dengel, A.C.; Griffith, W.P. Studies on transition-metal oxo and nitrido complexes. 12. Synthesis, spectroscopic properties, and reactions of stable ruthenium(V) and osmium(V) oxo complexes containing α-hydroxy carboxylate and α-amino carboxylate ligands. *Inorg. Chem.* **1991**, *30*, 869–871. [CrossRef]
21. Lei, Y.; Hurst, J.K. Dynamical investigations of the catalytic mechanisms of water oxidation by the $[(bpy)_2Ru(OH_2)]_2O^{4+}$ ion. *Inorganica Chim. Acta* **1994**, *226*, 179–185. [CrossRef]
22. Moonshiram, D.; Alperovich, I.; Concepcion, J.J.; Meyer, T.J.; Pushkar, Y. Experimental demonstration of radicaloid character in a Ru^V=O intermediate in catalytic water oxidation. *Proc. Natl. Acad. Sci.* **2013**, *110*, 3765–3770. [CrossRef] [PubMed]
23. Moonshiram, D.; Jurss, J.W.; Concepcion, J.J.; Zakharova, T.; Alperovich, I.; Meyer, T.J.; Pushkar, Y. Structure and electronic configurations of the intermediates of water oxidation in blue ruthenium dimer catalysis. *J. Am. Chem. Soc.* **2012**, *134*, 4625–4636. [CrossRef] [PubMed]
24. Duan, L.; Bozoglian, F.; Mandal, S.; Stewart, B.; Privalov, T.; Llobet, A.; Sun, L. A molecular ruthenium catalyst with water-oxidation activity comparable to that of photosystem II. *Nat. Chem.* **2012**, *4*, 418–423. [CrossRef] [PubMed]
25. Pushkar, Y.; Moonshiram, D.; Purohit, V.; Yan, L.; Alperovich, I. Spectroscopic analysis of catalytic water oxidation by $[Ru^{II}(bpy)(tpy)H_2O]^{2+}$ suggests that Ru^V=O is not a rate-limiting intermediate. *J. Am. Chem. Soc.* **2014**, *136*, 11938–11945. [CrossRef] [PubMed]
26. Moonshiram, D.; Purohit, V.; Concepcion, J.J.; Meyer, T.J.; Pushkar, Y. Mechanism of catalytic water oxidation by the ruthenium blue dimer catalyst: Comparative study in D_2O versus H_2O. *Materials* **2013**, *6*, 392–409. [CrossRef]
27. Yan, L.; Zong, R.; Pushkar, Y. Unexpected ligand lability in condition of water oxidation catalysis. *J. Catal.* **2015**, *330*, 255–260. [CrossRef]
28. Takeuchi, K.J.; Thompson, M.S.; Pipes, D.W.; Meyer, T.J. Redox and spectral properties of monooxo polypyridyl complexes of ruthenium and osmium in aqueous media. *Inorg. Chem.* **1984**, *23*, 1845–1851. [CrossRef]
29. Wasylenko, D.J.; Ganesamoorthy, C.; Kolvisto, B.D.; Henderson, M.A.; Berllnguette, C.P. Insight into water oxidation by mononuclear polypyridyl Ru catalysts. *Inorg. Chem.* **2010**, *49*, 2202–2209. [CrossRef] [PubMed]
30. Brown, D.G.; Sanguantrakun, N.; Schulze, B.; Schubert, U.S.; Berlinguette, C.P.; Wasylenko, D.J.; Ganesamoorthy, C.C.; Kolvisto, B.D.; Henderson, M.A.; Berllnguette, C.P.; et al. Unraveling the roles of the acid medium, experimental probes, and terminal oxidant, $(NH_4)_2[Ce(NO_3)_6]$, in the study of a homogeneous water oxidation catalyst. *J. Am. Chem. Soc.* **2010**, *49*, 2202–2209.
31. Concepcion, J.J.; Jurss, J.W.; Norris, M.R.; Chen, Z.; Templeton, J.L.; Meyer, T.J. Catalytic water oxidation by single-site ruthenium catalysts. *Inorg. Chem.* **2010**, *49*, 1277–1279. [CrossRef] [PubMed]